Outside the Unusual Cell Wall of the Hyperthermophilic Archaeon *Aeropyrum pernix* K1 [S]

Gianna Palmieri‡, Raffaele Cannio, Immacolata Fiume, Mosé Rossi§, and Gabriella Pocsfalvi‡¶

In contrast to the extensively studied eukaryal and bacterial protein secretion systems, comparatively less is known about how and which proteins cross the archaeal cell membrane. To identify secreted proteins of the hyperthermophilic archaeon *Aeropyrum pernix* K1 we used a proteomics approach to analyze the extracellular and cell surface protein fractions. The experimentally obtained data comprising 107 proteins were compared with the *in silico* predicted secretome. Because of the lack of signal peptide and cellular localization prediction tools specific for archaeal species, programs trained on eukaryotic and/or Gram-positive and Gram-negative bacterial signal peptide data sets were used. PSortB Gram-negative and Gram-positive analysis predicted 21 (1.2% of total ORFs) and 24 (1.4% of total ORFs) secreted proteins, respectively, from the entire *A. pernix* K1 proteome, 12 of which were experimentally identified in this work. Six additional proteins were predicted to follow non-classical secretion mechanisms using SecP algorithms. According to at least one of the two PSortB predictions, 48 proteins identified in the two fractions possess an unknown localization site. In addition, more than half of the proteins do not contain signal peptides recognized by current prediction programs. This suggests that known mechanisms only partly describe archaeal protein secretion. The most striking characteristic of the secretome was the high number of transport-related proteins identified from the ATP-binding cassette (ABC), tripartite ATP-independent periplasmic, ATPase, small conductance mechanosensitive ion channel (MscS), and dicarboxylate amino acid-cation symporter transporter families. In particular, identification of 21 solute-binding receptors of the ABC superfamily of the 24 predicted *in silico* confirms that ABC-mediated transport represents the most frequent strategy adopted by *A. pernix* for solute translocation across the cell membrane. ***Molecular & Cellular Proteomics 8:2570–2581, 2009.***

The archaea are a unique group of organisms that share properties with both the eukarya and bacteria. For a long time, archaeal life was considered to be limited to extreme environments such as high temperature, alkaline and acidic hot springs, anaerobic sediments, and highly saline environments. In the last decade, by the use of the archaeal 16 S rRNA gene as a molecular marker in microbial surveys (1), numerous mesophilic species have also been detected (2). Archaea have been found frequently and sometimes closely associated with bacterial and eukaryotic host cells, including humans. One of the most intriguing aspects of archaea is their unusual barrier between the inner cell material and the cellular environment, *i.e.* their cell membrane. Biosynthesis of archaeal cell wall has been a subject of interest for a long time. Most of the archaeal species characterized so far have a single chemically distinct cell membrane, which differs considerably from their eukaryotic and bacterial counterparts (3). The ether-type polar lipid surface is covered by a surface layer (S-layer)[1] composed of glycoproteins crystallized in regular two-dimensional lattices with hexagonal or tetragonal symmetry (4, 5). The structural characterization of the S-layer (6, 7) and S-layer-embedded archaeal cellular appendices such as flagella (8), pili, and hami (7, 9) associated with a diverse arsenal of cellular functions like motility, cell-cell communication, signaling, adherence, and nutrient uptake, has been the subject of an increasingly significant number of studies. Protein secretion mechanisms through this unusual cell membrane have been mainly addressed by way of comparative genomics studies (10–12) and by genomic identification and characterization of signal peptidases (13, 14). Archaeal extracellular and cell membrane proteins have been predicted because of the presence of a tripartite N-terminal signal motif essential for protein secretion and subsequently cleaved by signal peptidases from the protein (11, 14, 15). In archaea three different signal peptidases have been identified and characterized so far (13): signal peptidase I is responsible for the cleavage of secretory signal peptides from the majority of secreted proteins, class III signal peptidase is responsible for

From the Institute of Protein Biochemistry-National Research Council, 80131 Naples and § Department of Structural and Functional Biology, University of Naples Federico II, 80134 Naples, Italy

Received, January 8, 2009, and in revised form, May 1, 2009
Published, MCP Papers in Press, July 28, 2009, DOI 10.1074/mcp.M900012-MCP200

[1] The abbreviations used are: S-layer, surface layer; ABC, ATP-binding cassette; TRAP, tripartite ATP-independent periplasmic; Tat, twin arginine translocation; MscS, small conductance mechanosensitive ion channel; SP, signal peptide; V-type, vacuolar type; PDHC, pyruvate dehydrogenase complex; AARE, acyl amino acid-releasing enzyme; SBP, solute-binding protein; MRP, multiple resistance and pH adaptation.

processing signal peptides from preflagellins and some sugar-binding proteins (11), and signal peptide peptidase is responsible for the hydrolysis of signal peptides following protein secretion. No signal peptidase II homolog in archaea has been described to date. Four distinct pathways have been proposed for archaeal protein export: the main "Sec" system, the twin arginine translocation or "Tat" pathway (12), the ATP-binding cassette (ABC) transport system (16), and the type IV prepilin-like pathway (11). Moreover, proteins without signal peptides could also be secreted by using nonspecific and/or currently unknown mechanisms. Despite the similarities in protein translocation mechanisms between the three domains of life, genome analyses also shed light on unique archaeal characteristics, suggesting that our current knowledge regarding secreted proteins and secretion mechanisms in archaea remains limited (10). It is apparent that the lack of experimental data at the proteome level has become the bottleneck for the further understanding of the existence of novel secretion mechanisms in archaea (15).

To date, the genome sequences of eight hyperthermophiles, including the crenarchaeon *Aeropyrum pernix* K1, have been determined. *A. pernix* K1, isolated from a coastal solfataric thermal vent on the Kodakara-Jima Island in Japan (17), is the first reported obligate aerobic and neutrophilic hyperthermophilic archaeon with an optimal growth temperature between 90 and 95 °C. The spherical shaped cells of *A. pernix* are ~1 μm in diameter, lack a rigid cell wall, and are covered by an S-layer with hexagonal symmetry. *A. pernix*, like other extreme thermophiles and acidophiles, possesses a particularly thick cell membrane that acts as a protective barrier, conferring to it the ability to function in the extreme environment in which it thrives. The lipids of *A. pernix* are different from those of anaerobic sulfur-dependent hyperthermophiles; they lack tetraether lipids and the direct linkage of inositol and sugar moieties (18). *A. pernix* K1 contains a 1.6-Mbp chromosome that has been sequenced; it comprises 1700 annotated genes. By using different proteomics approaches, the proteome of *A. pernix* K1 has recently been analyzed, leading to the identification of 704 proteins (41% of total ORFs) (19). In this work we performed proteomics analysis of the cell surface and extracellular protein fractions purified from *A. pernix* K1 to define proteins targeted to the cell secretome. We also analyzed the complete predicted proteome of *A. pernix* K1 by *in silico* signal peptide and cellular localization prediction tools and compared the experimentally obtained data set with the predicted secretome.

EXPERIMENTAL PROCEDURES

Culture Condition—*A. pernix* K1 (JCM 9820) was grown at 90 °C in a 10-liter fermenter in marine broth (Difco) (37.4 g/liter) and sodium thiosulfate (10 g/liter) as described (17). Cells were harvested at the middle exponential growth phase (0.5 A_{600}). 1 liter of culture was used to prepare the two protein fractions. Cells were collected by centrifugation at 2000 × *g* at 4 °C for 30 min and used to prepare the surface fraction. The supernatant was filtered (0.45 μm) and used to prepare the exoprotein fraction. Three independent cultures were performed under the same conditions, and the resulting biological samples were processed independently.

Extraction of Surface Protein Fraction—Cells were washed in 20 mM Tris-HCl, pH 6.5 and resuspended in the same buffer containing 0.7 mM PMSF. Cells were lysed by sonication (eight cycles, 15-s pulse on and 45-s pulse off) using a Soniprep (B. Braun Labsonic U) equipped with a microprobe. Unbroken cells were removed by centrifugation at 2000 × *g* at 4 °C for 20 min. Membranes were collected by ultracentrifugation of the supernatant at 100,000 × *g* at 4 °C for 45 min. The pellet was washed four times with 20 mM Tris HCl, pH 6.5; resuspended in 20 mM Tris-HCl, pH 6.5; and solubilized in the presence of 1% Triton X-100 and 0.7 mM PMSF at 37 °C for 30 min. Insoluble material was removed by centrifugation at 250,000 × *g* at 4 °C for 15 min. The pellet was washed three times with the same buffer, and the collected supernatant containing the surface membrane proteins was harvested and extensively dialyzed against 20 mM Tris-HCl, pH 8.0 and 0.2% Triton X-100.

Extraction of Extracellular Protein Fraction—Proteins were precipitated from the filtered culture medium by the addition of $(NH_4)_2SO_4$ up to 80% saturation at 4 °C. The sample was centrifuged at 12,000 × *g* at 4 °C for 30 min. The precipitate was resuspended in 25 mM Tris-HCl, pH 8.0; extensively dialyzed against the same buffer; and concentrated by an Amicon stirred ultrafiltration cell (Millipore) using a PM-10 membrane.

One-dimensional SDS-PAGE Separation and Peptide Extraction—Protein concentrations were determined by the Bradford method using the Bio-Rad protein staining assay. Samples (30 μg) were dissolved in 20 μl of 125 mM Tris-HCl, pH 6.8, 4% SDS, 20% glycerol, 0.2 M DTT, and 0.02% bromphenol blue; boiled at 100 °C for 5 min; and loaded on a 12.5% polyacrylamide gel (10 × 7 cm) (20). Electrophoresis was carried out using 25 mM Tris, 192 mM glycine, and 0.1% SDS at 15 mA/gel. The gel was fixed and stained with Coomassie Brilliant Blue G-250. The resulting gel lanes were sequentially cut into 25 slices (3 mm each) manually, and protein in-gel digestion (21) was performed using 30 μl of 10 mM DTT in 100 mM NH_4HCO_3 and 5% ACN for reduction, 30 μl of 55 mM iodoacetamide in 100 mM NH4HCO3 for alkylation, and 30 μl of trypsin (Promega) at 6 ng/μl in 50 mM NH_4HCO_3 and 10% ACN.

Nano-HPLC-ESI-MS/MS Analysis—Tryptic peptides were analyzed using a Q-TOF instrument, QSTAR Elite (Applied Biosystems, Foster City, CA) equipped with a nanoflow electrospray ion source. A pulled silica capillary (170-μm outer diameter; 100-μm inner diameter; tip, 30-μm inner diameter) was used as the nanoflow tip. The samples (1–10 μl of 40 μl) were loaded, purified, and concentrated on a precolumn (PepMap, C_{18}, 5-mm length, 300 Å; LCPackings, Sunnyvale, CA) at a 30 μl/min flow rate. Peptide separation was performed by Ultimate 3000 (Dionex, Sunnyvale, CA) using a capillary column (PepMap, C_{18}, 15-cm length, 75-μm inner diameter, 300 Å; LCPackings). Solvent A was 2% ACN in 0.1% formic acid (HCOOH) and 0.025% TFA, and solvent B was 98% ACN in 0.1% HCOOH and 0.025% TFA at a 300 nl/min flow rate. The following gradient was used: 5–50% B in 30 min, 50–98% B in 6 s. CID experiments were carried out in information-dependent analysis mode using nitrogen as the collision gas. Two independent nano-HPLC-ESI-MS/MS experiments were performed for each sample.

Database Search—Tandem mass spectra were extracted, and peak lists were generated by Analyst QS 2.0 software using the default parameters. Peak lists containing all acquired MS/MS spectra were analyzed using Mascot Server (version 2.2) and X! Tandem (The Global Proteome Machine Organization; version 2007.01.01.1). Peak lists deriving from the two independent nano-HPLC-ESI-MS/MS runs were summed into a unique peak list. Mascot Server was set up to search the NCBInr-extracted *A. pernix* K1 database containing 1700

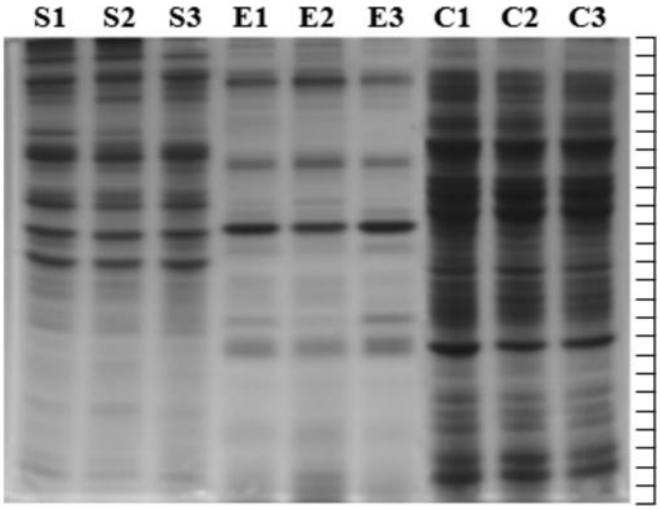

FIG. 1. **SDS-PAGE image of surface (*lanes S1*, *S2*, and *S3*), exoprotein (*lanes E1*, *E2*, and *E3*), and cytosolic (*lanes C1*, *C2*, and *C3*) protein fractions isolated in the middle exponential growth phase of *A. pernix* K1 in three independent experiments.** Gel lanes were cut into 25 3-mm pieces for proteomics analyses. Identified proteins in the surface and exoprotein fractions are listed in Tables I and II, respectively.

entries. Trypsin was specified as the digestion enzyme with a maximum of one missed cleavage site. X! Tandem was set up to search the same database. Mascot and X! Tandem were run with a fragment ion mass tolerance of 0.08 Da and a parent ion tolerance of 50 ppm. The carbamidomethyl derivative of cysteine was specified as a fixed modification, whereas oxidation of methionine was specified as a variable modification in Mascot and X! Tandem searches. Acetylation of the N terminus was specified in X! Tandem as a variable modification.

Criteria for Protein Identification—Scaffold (version Scaffold_2_02_03, Proteome Software Inc., Portland, OR) was used to validate MS/MS-based peptide and protein identifications. Peptide identifications were accepted at greater than 95.0% probability as specified by the PeptideProphet algorithm (22). Protein identifications were accepted at greater than 99.0% probability if they contained at least three identified peptides.

Prediction Tools—SignalP 3.0 (23), SecretomeP 2.0 (24), TatP 1.0 (25), LipoP 1.0 (26), TMHMM 2.0 (27), PSortB v.2.0 (28), FlaFind 1.0 (11), TATFIND 1.4 (29), and Duf361-Like 1.0 (11) were used. The FASTA format of the genome-translated proteome of *A. pernix* K1 consisting of 1700 predicted protein sequences was used as the input.

RESULTS

Membrane Surface Proteins of A. pernix K1—Here we carried out a proteomics analysis to identify proteins present on the cell surface of *A. pernix* K1. Preparation of the cell surface fraction was based on the differential centrifugation and solubilization of cell membranes obtained after lysis; thus both outer and inner membrane-associated proteins were expected to be present in this fraction. In total 89 unique proteins were identified with high confidence (Fig. 1, Table I, and supplemental Table 1). S-layer protein (APE_0609.1), usually the most abundant integral membrane protein, was identified with a low probability in the surface fractions, indicating that the samples were not significantly contaminated with integral membrane proteins. A flagellin homolog, APE_1907, namely a component of the appendices embedded to the outer cell surface, could be identified.

One of the most striking features of the surface fraction was the high number of substrate-binding components of transport-related proteins belonging to the ABC and tripartite ATP-independent periplasmic (TRAP) systems (Table I and supplemental Table 1). Interestingly, four subunits of vacuolar (V)-type ATPases, namely subunits A, B, D, and E, were also identified. Evidence is growing that in the ancestor ATPase ATP hydrolysis was coupled to the transfer of RNA and/or proteins across the cell membrane (30). This theory is supported by the homology observed between ATPases (F- and V-types) and the bacterial flagellar motors secreted by type III secretion systems that are also responsible for the secretion of some ABC transporters in archaea. The following proteins, which could be putatively involved in cellular trafficking, were also expressed: hypothetical protein APE_1719.1, a putative maltose ABC transporter; proton glutamate symport protein (APE_2583.1) from the dicarboxylate amino acid-cation (H^+) symporter secondary transporter family; small conductance mechanosensitive channel MscS protein (APE_1867.1) from the ion channel transporter family; hypothetical protein APE_0061.1; and the membrane lipoprotein APE_2592.1. The last two have a common conserved domain of the periplasmic binding protein type 1 superfamily that is related to the surface lipoprotein component of an uncharacterized ABC-type transporter.

Numerous respiratory pathway-related proteins were found in the surface fraction. Among these, the arsenite oxidase large subunit was identified. This protein has been characterized in both chemolithoautotrophic and heterotrophic bacteria as coupled to alternative respiration pathways, including nitrate reduction, and/or as involved in energy-producing redox processes (31). More intriguingly, an unexpectedly high amount of nitrate reductase complex represented by three subunits, α (APE_1288.1), β APE_1294.1), and putative γ (APE_1297), was identified in several gel slices over the one-dimensional SDS-PAGE lanes (Fig. 1). In addition, a number of proteins putatively responsible for the regulation of aerobic cellular respiration within the cell membrane, like Rieske iron-sulfur protein, NADH dehydrogenase (subunits D and I), NuoB and NuoC homologs, succinate dehydrogenase iron-sulfur and flavoprotein subunits, were also expressed. Regarding the nitrate-reducing enzyme, there are three different systems described in prokaryotes: the cytoplasmic assimilatory (Nas), the membrane-bound anaerobic respiratory (Nar), and the periplasmic (Nap) systems (32). Most nitrate-reducing archaea use nitrate as an alternative electron acceptor in anaerobic respiration; nevertheless the nitrate reduction pathway is found also in both strict and facultative aerobic genera. In fact, Nar enzymes have been purified from denitrifying archaea such as some aerobic halophilic euryarchaeota (17).

TABLE I
Proteins identified in the membrane surface fraction of A. pernix K1

Protein name	Accession number	ORF	Molecular mass	Unique peptides	Unique spectra	Total spectra	Sequence coverage
			Da				%
Nitrate reductase, α subunit	gi|118431398	APE_1288.1	145,341.7	68	78	1,115	56.70
Oligopeptide ABC transporter, oligopeptide-binding protein	gi|118431519	APE_1583.1	101,753.3	36	47	914	50.90
ABC transporter, substrate-binding protein	gi|118431538	APE_1630.1	52,222.9	23	30	708	61.40
Nitrate reductase, β subunit	gi|118431399	APE_1294.1	53,617.9	31	34	647	64.00
TRAP transporter, solute-binding component	gi|118431744	APE_2136.1	35,017.4	18	24	414	64.10
Branched chain amino acid ABC transporter, branched chain amino acid-binding protein	gi|14601070	APE_0917	53,601.3	25	28	377	48.00
Probable ABC transporter, substrate-binding protein	gi|118431798	APE_2254.1	64,664.7	34	38	369	57.70
Dipeptide ABC transporter, dipeptide-binding protein DppA	gi 14601949	APE_2257	57,903.5	16	18	174	31.50
V-type ATP synthase subunit A	gi|118431026	APE_0405.1	66,953.4	33	34	157	57.10
TRAP transporter, solute-binding component	gi|118431921	APE_2545.1	39,903.0	13	16	154	47.70
ABC transporter, substrate-binding protein	gi|118431437	APE_1390.1	83,897.1	21	24	136	37.80
Hypothetical protein APE_0969.1	gi|118431278	APE_0969.1	42,426.3	5	8	123	16.80
V-type ATP synthase subunit B	gi|118431025	APE_0404.1	51,615.4	15	16	116	41.00
ABC transporter, substrate-binding protein	gi|118430849	APE_0035.1	52,225.7	12	12	87	42.10
Putative ABC transporter, substrate-binding protein	gi|118431313	APE_1049.1	52,379.7	15	21	92	42.40
Branched chain amino acid ABC transporter, branched chain amino acid-binding protein	gi|118431910	APE_2521.1	47,195.2	15	19	81	46.40
Erythrocyte band 7 integral membrane protein homolog	gi|118431753	APE_2153.1	30,551.8	10	10	50	37.30
Cell division control protein 48, AAA family	gi|118431889	APE_2239.1	82,109.5	16	16	27	23.70
Putative nitrate reductase, γ subunit	gi|14601316	APE_1297	33,976.3	4	5	61	19.00
Hypothetical protein APE_0061.1	gi|118430860	APE_0061.1	47,933.7	17	17	48	56.20
Hypothetical protein APE_0966.1	gi|118431277	APE_0966.1	78,471.3	16	16	43	25.80
Spermidine/putrescine ABC transporter, spermidine/putrescine-binding protein	gi|118431267	APE_0945.1	44,149.2	7	9	42	24.30
Phosphate ABC transporter, phosphate-binding protein	gi|14600404	APE_0045	40,287.3	11	11	47	39.90
V-type ATP synthase subunit D	gi|118431024	APE_0402.1	24,695.4	10	10	31	46.40
Putative dehydrogenase	gi|14602197	APE_1043.1	41,853.9	7	7	26	22.60
Hypothetical protein APE_1719.1	gi|118431565	APE_1719.1	20,363.0	3	3	31	14.20
ABC transporter, substrate-binding protein	gi|118430987	APE_0304.1	90,222.4	16	16	30	23.80
Succinate dehydrogenase flavoprotein subunit	gi|118431269	APE_0950.1	65,561.1	14	14	31	27.10
NADH dehydrogenase subunit I	gi|118431451	APE_1419.1	21,306.5	7	7	26	32.30
Succinate dehydrogenase iron-sulfur subunit	gi|14601092	APE_0946	34,672.0	10	10	30	31.50
Branched chain α-keto acid dehydrogenase subunit E2	gi|14601549	APE_1371	44,963.5	13	14	28	45.60
Branched chain amino acid ABC transporter, ATP-binding protein	gi|14601072	APE_0921	26,411.1	10	10	20	49.40
Flagellin homolog	gi|14601713	APE_1907	25,923.3	3	3	20	19.90
V-type ATP synthase subunit E	gi|118431027	APE_0409.1	22,124.3	5	6	14	33.50
Surface layer-associated protease precursor	gi|14600834	APE_0607	142,047.9	11	11	20	11.00
Hypothetical protein APE_2352.1	gi|118431843	APE_2352.1	35,202.2	8	8	20	28.70
Oligopeptide ABC transporter, ATP-binding protein	gi|14601497	APE_1578	35,711.1	7	7	19	26.90
Pyruvate dehydrogenase E1 component, β subunit	gi|14601550	APE_1674	36,590.0	7	7	13	24.30
Branched chain amino acid ABC transporter, ATP-binding protein	gi|14601071	APE_0919	27,846.0	9	9	17	38.60
Surface layer protein	gi|118431124	APE_0609.1	164,494.4	3	4	17	3.16
Hypothetical protein APE_1758.1	gi|118431578	APE_1758.1	53,456.3	10	11	16	29.10
Hypothetical protein APE_1406.1	gi|118431442	APE_1406.1	37,745.2	8	9	16	25.70
Hypothetical protein APE_1117	gi|14601190	APE_1117	25,867.9	6	6	17	36.80

TABLE I—*continued*

Protein name	Accession number	ORF	Molecular mass	Unique peptides	Unique spectra	Total spectra	Sequence coverage
			Da				%
ABC transporter, substrate-binding protein	gi|118431555	APE_1688.1	30,468.1	6	6	15	28.80
DNA repair and recombination protein RadA	gi|14600463	APE_0119	35,302.8	7	7	16	25.10
Hypothetical protein APE_2146.1	gi|118431749	APE_2146.1	43,603.1	5	5	14	12.40
NADH dehydrogenase subunit D	gi|14601398	APE_1422	46,622.6	8	8	12	23.40
Oligopeptide ABC transporter, ATP-binding protein	gi|14601496	APE_1576	42,614.0	5	5	13	23.30
Hypothetical protein APE 1973.1	gi|118431669	APE 1973.1	72,812.3	5	5	15	9.67
MRP/NBP35 family protein	gi|118430945	APE_0230.1	33,704.7	7	7	13	22.30
Replication factor C small subunit	gi|118431491	APE_1522.1	37,327.2	7	7	13	25.80
Hypothetical protein APE_2212.1	gi|118431782	APE_2212.1	32,323.1	7	7	13	28.40
Probable arsenite oxidase large subunit	gi|118431923	APE_2556.1	113,264.6	7	7	10	9.24
50 S ribosomal protein L4P	gi|118430943	APE_0228.1	30,198.2	9	9	12	35.70
Dihydrolipoyl dehydrogenase	gi|118431550	APE_1669.1	48,851.8	8	8	10	23.30
DNA double strand break repair rad50 ATPase	gi|14600457	APE_0110	104,126.6	4	4	6	7.83
Hypothetical protein APE_0558.1	gi|118431107	APE_0558.1	45,254.5	5	5	10	20.40
Membrane lipoprotein family protein	gi|118431933	APE_2592.1	48,132.8	5	5	11	12.10
Fibrillarin	gi|14601907	APE_2196	26,682.4	4	4	10	19.70
ABC transporter, substrate-binding protein	gi|118431638	APE_1893.1	30,607.6	4	4	11	13.80
Proton glutamate symport protein	gi|118431930	APE_2583.1	44,583.3	4	4	9	9.91
Molybdopterin oxidoreductase, molybdopterin binding subunit	gi|14602175	APE_2610	131,525.6	6	6	9	5.24
Rieske iron-sulfur protein	gi|118431568	APE_1724.1	28,721.7	3	4	10	17.00
ABC transporter, substrate-binding protein	gi|118431402	APE_1303.1	46,381.4	5	5	9	15.20
Pyruvate dehydrogenase E1 component, α subunit	gi|118431551	APE_1677.1	42,305.0	7	7	7	21.50
Proteasome β subunit	gi|118431082	APE_0507.1	21,569.0	5	6	8	26.10
Hypothetical protein APE_1868.1	gi|118431625	APE_1868.1	27,454.8	5	5	8	23.50
NuoC homolog	gi|14601399	APE_1426	21,286.7	4	4	8	23.80
Translation initiation factor IF 2 subunit α	gi|118431043	APE_0436.1	31,460.9	5	5	5	17.30
NuoB homolog	gi|118431453	APE_1428.1	22,131.4	5	5	7	29.60
Long chain fatty acid-CoA ligase	gi|118431813	APE_2284.1	61,293.6	4	4	5	10.40
Putative ABC transporter, ATP-binding protein	gi|118431315	APE_1055.1	27,089.9	4	4	6	12.40
Cell division control protein 48, AAA family	gi|14601365	APE_1367	81,228.8	3	3	4	9.23
Thermosome α subunit	gi|118431257	APE_0907.1	60,357.7	5	5	5	10.10
Hypothetical protein APE_1123.1	gi|118431334	APE_1123.1	41,032.8	5	5	5	16.40
Proteasome subunit α	gi|14601414	APE_1449	28,822.0	5	5	6	23.30
2-Oxoglutarate ferredoxin oxidoreductase subunit β	gi|14601428	APE_1472	34,393.8	5	5	5	18.10
Hypothetical protein APE_2139.1	gi|118431745	APE_2139.1	23,962.9	4	4	5	19.30
Oligopeptide ABC transporter, permease protein	gi|14601499	APE_1582	40,673.6	4	4	6	9.92
Hypothetical protein APE_0145	gi|14600482	APE_0145	27,638.4	3	3	6	10.60
δ-Aminolevulinic acid dehydratase	gi|118431821	APE_2300.1	38,718.6	4	4	4	13.30
Hypothetical protein APE_1952.1	gi|118431658	APE_1952.1	51,685.3	4	4	5	9.94
Small conductance mechanosensitive channel MscS	gi|118431624	APE_1867.1	30,693.9	3	3	4	13.30
Acetyl-CoA acetyltransferase	gi|14602032	APE_2384	43,437.6	3	4	4	11.40
Acidic ribosomal protein P0	gi|118431764	APE_2171.1	37,255.8	4	4	4	20.50
50 S ribosomal protein L2P	gi|14600538	APE_0218	25,723.3	4	4	4	21.40
Thioredoxin	gi|14600860	APE_0641	37,064.9	3	3	4	10.00
Hypothetical protein APE_2435	gi|14602061	APE_2435	29,134.1	3	3	3	11.80
Putative oxidoreductase, aldo/keto reductase family	gi|14601541	APE_1659	36,170.6	3	3	3	14.30

To our knowledge this is the first evidence of a high level expression at the protein level of nitrate reductase during aerobic growth together with the parallel oxygen-based respiratory protein complex. The absence of the usual switch-off of the respiratory mode relying on nitrate as the electron acceptor in aerobic growth raises the question whether

A. pernix is a real, strict aerobic microorganism and/or whether the growth conditions at 90 °C can be considered aerobic. In fact, the amount of nitrate (0.02 mM) in the optimal growth medium of *A. pernix* cannot be considered sufficient to sustain anaerobic alternative respiration. Moreover, oxygen solubilization decreases about 10 times at 90 °C when compared with that at room temperature (from 200 to 20 μM). Therefore, the growth conditions of *A. pernix* can be rewarded as microaerophilic rather than strictly aerobic. More detailed studies of the respiratory modes of *A. pernix*, both at the transcriptome and proteome levels under different growth conditions in the alternative presence of electron acceptors, such as oxygen and nitrate, are currently underway.

Subunits of large inner membrane-associated multisubunit protein complexes like the ribosome, thermosome, and pyruvate dehydrogenase were also detected in the cell surface fraction. In particular, three subunits of 50 S ribosome, L2P, L4P, and P0, were identified. Ribosomal proteins are often considered as contaminants of membrane preparations. However, in archaea up to half of the ribosomes is known to be attached to the cell membrane by a specific interaction between the signal recognition particle and the ribosome (33, 34). Membrane-binding ribosomes are believed to have an important role in the general co-translational protein translocation system of archaea. Experimental evidence of co-translational membrane protein insertion has recently been described for *Haloferax volcanii* (33).

A. pernix K1 has two genes encoding the putative thermosome subunits α and β (35); the α subunit was identified in this fraction. The thermosome is known to function as part of a protein folding system in the cytoplasm and is expected to be highly expressed in *A. pernix* as it is in the hyperthermophilic archaeon *Sulfolobus shibatae*. Interestingly, the two subunits have also been shown to form membrane-associated rosettasomes as well as ordered bundled filaments and have been proposed to act as a kind of membrane skeleton in *S. shibatae* (36). Therefore, it was supposed that the thermosome may not have been merely the consequence of cytosolic contamination.

Pyruvate dehydrogenase complex (PDHC) is a multienzyme complex consisting of multiple copies of three component enzymes. PDHC is often inner membrane-associated in mitochondria, chloroplasts, and bacteria. Two proteins of the E1 component (α and β subunits) and one from the E2 component (APE_1371) of this complex were identified.

Exoproteins of A. pernix K1—Proteins secreted into the extracellular medium in the middle exponential cellular growth phase were analyzed. *A. pernix* K1 secretes a relatively high amount of proteins into the culture medium (4.2 mg/liter of culture at 0.5 A_{600}). Extracted proteins were separated by one-dimensional SDS-PAGE (Fig. 1), and the resulting 25 gel slices were subjected to nano-HPLC-ESI-MS/MS analysis. In this fraction 40 unique proteins were identified with high confidence (Table II). The relatively low number of identified proteins compared with what is usual in the exoprotein fractions of bacteria (37) and eukarya suggests that the secretome of *A. pernix* is less complex. There are 22 proteins that overlap with those already identified in the surface protein fraction (Table I) pertaining mainly to the molecular transport systems, *i.e.* the various solute-binding components of ABC and TRAP transporters, two components of an uncharacterized ABC-type transporter (APE_2592.1 and APE_0966.1), and the molybdopterin binding subunit of the molybdopterin oxidoreductase. In addition, α and β subunits of the nitrate reductase complex, surface layer protein, surface layer-associated protease, and four hypothetical proteins (APE_1117, APE_0061.1, APE_0558.1, and APE_ 1952.1) were identified in both fractions.

The most significant feature of the extracellular fraction (Table II) was the presence of a high number of enzymes that are mainly involved in the degradation of polypeptides. This may be particularly interesting because most archaea research is focused on the identification and characterization of specific enzymes that exhibit highly specific activity under extreme conditions. Among the most abundant proteins, two predicted proteases, protease I (APE_0319) and surface layer-associated protease, were identified. Protease I is a small, 180-amino acid-long (molecular mass, 20 kDa) protein with a type 1 glutamine amidotransferase-like domain. Type 1 glutamine amidotransferases are ATP-independent intracellular proteases that hydrolyze small peptides to provide a nutritional source. The extracellular proteolytic activity of the hyperthermophilic archaeon *Pyrococcus furiosus* has been attributed to a homolog of type 1 glutamine amidotransferase protein (PfpI), which has been shown to form homomultimers in solution even under denaturing conditions (38). Protease I was identified in various gel slices in the extracellular fraction but also in the cytoplasmic fraction of *A. pernix* (data not shown). The high expression level of this putative protease in *A. pernix* K1 makes it an interesting target for further enzymatic characterization. S-layer-anchored protease, on the other hand, is a high molecular mass (142-kDa) putative subtilisin serine protease that was identified in both the surface and extracellular fractions. Pernisine, another recently characterized extracellular subtilisin-like serine protease of *A. pernix* (39), was also identified in this work.

Acyl amino acid-releasing enzyme (AARE; APE_2290.1) liberates the N-terminal acetyl amino acid from *N*-acetylated peptides. It has been suggested that AARE affects the cellular processing and sorting mechanisms in eukaryotic cells. AARE has been purified and characterized from a number of archaea, including *A. pernix* (40).

Leucine aminopeptidase (APE_2450.1, band 1) is a probable exopeptidase. Leucine aminopeptidase is a member of the M17 family of peptidases that catalyze the removal of amino acids from the N terminus of a protein. Leucine aminopeptidase plays a key role in protein degradation. It is called leucine aminopeptidase because it reacts most rapidly at a

TABLE II
Proteins identified in the exoprotein fraction of A. pernix K1

Protein name	Accession number	ORF	Molecular mass	Unique peptides	Unique spectra	Total spectra	Sequence coverage
			Da				%
Oligopeptide ABC transporter, oligopeptide-binding protein	gi|118431519	APE_1583.1	101,753.3	67	85	1,559	67
5′-Methylthioadenosine phosphorylase II	gi|14601697	APE_1885	30,718.8	20	20	42	70
Hypothetical protein APE_1457	gi|14601419	APE_1457	19,640.5	3	3	3	18
Hypothetical protein APE_1117	gi|14601190	APE_1117	25,867.9	26	28	164	94
Acylamino acid-releasing enzyme	gi|118431816	APE_2290.1	70,202.4	34	36	59	62
Hypothetical protein APE_0061.1	gi|118430860	APE_0061.1	47,933.7	17	19	55	47
Δ^1-Pyrroline-5-carboxylate dehydrogenase	gi|118431207	APE_0807.1	61,654.6	10	10	10	28
ABC transporter, substrate-binding protein	gi|118430849	APE_0035.1	52,225.7	7	7	29	18
ABC transporter, substrate-binding protein precursor	gi|118430987	APE_0304.1	90,222.4	7	7	17	10
Nitrate reductase, β subunit	gi|118431399	APE_1294.1	53,617.9	16	16	39	33
Nitrate reductase, α subunit	gi|118431398	APE_1288.1	145,341.7	36	36	96	32
Thiosulfate sulfurtransferase	gi|118431935	APE_2595.1	33,219.3	6	6	8	19
Membrane lipoprotein family protein	gi|118431933	APE_2592.1	48,132.8	11	11	15	29
ABC transporter, substrate-binding protein precursor	gi|118431437	APE_1390.1	83,897.1	32	35	212	54
Aldehyde dehydrogenase, large subunit	gi|118431783	APE_2216.1	85,738.9	26	27	48	41
Hypothetical protein APE_0558.1	gi|118431107	APE_0558.1	45,254.5	3	3	3	12
Dipeptide ABC transporter, dipeptide-binding protein DppA	gi|14601949	APE_2257	57,903.5	17	18	49	31
Aspartate aminotransferase	gi|14602053	APE_2423	41,244.7	6	6	6	17
ABC transporter, substrate-binding protein	gi|14601589	APE_1728	56,773.1	13	13	50	22
Hypothetical protein APE_0338.1	gi|118431004	APE_0338.1	49,550.3	32	32	53	58
Surface layer protein	gi|118431124	APE_0609.1	164,494.4	34	37	83	22
ABC transporter, substrate-binding protein	gi|118431402	APE_1303.1	46,381.4	4	4	14	14
Leucine aminopeptidase	gi|118431875	APE_2450.1	52,370.8	17	17	35	41
Protease I	gi|14600627	APE_0319	20,028.3	24	30	254	88
Aldehyde dehydrogenase, large subunit	gi|118431161	APE_0708.1	83,856.3	34	35	67	50
Branched chain amino acid ABC transporter, branched chain amino acid-binding protein	gi|14601070	APE_0917	53,601.3	27	30	231	52
Surface layer-associated protease precursor	gi|14600834	APE_0607	142,047.9	30	30	32	29
Phosphate ABC transporter, phosphate-binding protein	gi|14600404	APE_0045	40,287.3	7	7	11	27
Pernisine	gi|118430960	APE_0263.1	43,695.7	3	3	5	10
Molybdopterin oxidoreductase, molybdopterin binding subunit	gi|14602175	APE_2610	131,525.6	3	3	4	3
Aldehyde dehydrogenase, small subunit	gi|14601917	APE_2213	17,845.2	5	5	13	37
Hypothetical protein APE_0858	gi|14601024	APE_0858	59,001.4	9	9	9	28
Hypothetical protein APE_1952.1	gi|118431658	APE_1952.1	51,685.3	12	12	20	23
Probable ABC transporter, substrate-binding protein	gi|118431798	APE_2254.1	64,664.7	38	44	276	62
Hypothetical protein APE_0966.1	gi|118431277	APE_0966.1	78,471.3	11	11	20	17
Putative hydrolase	gi|118431842	APE_2350.1	23,362.6	12	12	13	70
Branched chain amino acid ABC transporter, branched chain amino acid-binding protein	gi|118431910	APE_2521.1	47,195.2	9	9	10	20
TRAP transporter, solute-binding component	gi|118431744	APE_2136.1	35,017.4	22	26	49	59
Aldehyde dehydrogenase, middle subunit	gi|14601920	APE_2219	31,568.7	27	29	53	74
Hypothetical protein APE_2446	gi|14602070	APE_2446	39,002.9	5	5	5	15

leucine site. The molecular mass of this enzyme is lower (52 kDa) than one can expect from its appearance on the SDS-PAGE gel. This may suggest the formation of an extremely stable multimeric assembly.

Other identified enzymes were metal-dependent hydrolase (APE_1117), 5′-methylthioadenosine phosphorylase II (APE_1885), aspartate aminotransferase (APE_2423), Δ^1-pyrroline-5-carboxylate dehydrogenase (APE_0807.1), and thiosulfate sulfurtransferase (APE_2595.1). Functional roles of most of these enzymes in archaea still await more detailed characterization.

DISCUSSION

Comparison of in Silico and Proteomics Results—The predicted *A. pernix* K1 proteome based upon the *in silico* translation of the completed genome (41), consisting of 1700 entries, was submitted to signal peptide and cellular localization prediction algorithms. It should be noted that the majority of these methods were trained and validated on eukaryotic and/or Gram-negative and Gram-positive prokaryotes; therefore, their applications to archaeal species by some means are limited. Results obtained are listed in supplemental Table 3 and summarized in Fig. 2.

SignalP, based on a neural network and hidden Markov model (23), was used to predict the presence of signal peptide 1 (SP1). According to eukaryotic SignalP predictions 256 proteins (corresponding to 15% of total ORFs) possess a putative secretory SP1. Considerably fewer, 102 and 116 proteins, turned out to be positive by Gram-negative and Gram-positive SignalP calculations. The 278 proteins (16%) that were positive at least for one of the three SignalP predictions were considered to be potentially exported by the Sec-dependent pathway (Fig. 2). This set includes putative membrane-bound proteins besides those secreted outside the cell wall. Putative Tat signal peptides were predicted by TatP (25) and TATFIND (29), respectively. Tat signal peptides are involved in Sec-independent protein targeting, which is dedicated to the export of folded proteins. In the Tat-dependent export, proteins harboring a distinctive N-terminal signal peptide containing the "twin arginine" amino acid motif with SRR*X*FLK consensus are targeted to the Tat translocase. Based on bacterially trained TatP prediction 11 proteins have a Tat motif, and 26 proteins have a potential Tat signal peptide without Tat motif. The more stringent TATFIND program, chiefly trained by using the sequences of putative haloarchaeal Tat signal peptides, predicted nine proteins of which four were already positive for TatP. Proteins that were positive for at least one of the two Tat prediction tools (16 proteins) were considered as potential substrates of the Tat translocation system (Fig. 2). To predict archaeal class III signal peptides (SP3) and their prepilin peptidase cleavage sites, FlaFind and Duf361-Like programs were used. Based on FlaFind, 18 proteins were found to have a putative SP3, whereas no protein with a DUF361-like domain was predicted in the proteome of *A. pernix* K1.

Subcellular protein localization was predicted by the open source PSortB program (28). PSortB uses support vector machine-based classification and was trained on bacterial prokaryotic systems. PSortB analyzes different aspects like homology to proteins of known localization, amino acid composition, the presence of signal peptides, sequence motifs, and transmembrane helices. The program predicts five Gram-negative (*i.e.* cytoplasm, membrane, periplasm, outer membrane, and extracellular) and four Gram-positive (*i.e.* cytoplasm, membrane, cell wall, and extracellular) subcellular localizations. Extracellular, outer membrane, periplasmic, and cell wall proteins in this work were considered as the potential secretome. Predicted localization sites of *A. pernix* K1 proteins calculated by PSortB (supplemental Table 3) are shown in Fig. 2. Only 21 secreted proteins (1.2% of total ORFs) were predicted based on Gram-negative calculations, and slightly more, 24 (1.4% of total ORFs) proteins, were predicted based on Gram-positive calculations. A high number of proteins (15 and 35% of the total ORFs) were found to have an "unknown" localization site, whereas most of the non-cytoplasmic proteins were predicted to be membrane-localized (15 and 17%) because of the identification of three or more transmembrane helices by the program.

In this work the "experimental secretome" of *A. pernix* is defined as the sum of identified exo- and outer surface proteins. The surface protein fraction analyzed, however, comprises both outer and inner surface-bound proteins and as well as some integral membrane protein contamination (89 proteins; Table I). Therefore, in the first instance, inner surface-localized proteins and proteins with more than three transmembrane helices (integral membrane proteins) were subtracted from this set. These were the seven subunits of large multisubunit protein complexes (thermosome, ribosome, and PDHC), five ATP-binding proteins from ABC transporter systems, and four integral membrane proteins (*i.e.* hypothetical protein APE_1973.1, proton glutamate symport protein, oligopeptide ABC transporter, permease protein APE_1582, and hypothetical protein APE_2435). For the 13 inner surface predicted proteins no signal peptides and transmembrane helices were identified (supplemental Table 4B). The remaining 73 proteins identified in the surface fraction (Table I) and the 40 exoproteins identified in the exoprotein fraction (Table II) containing 91 unique proteins (supplemental Table 4A) were analyzed by the same prediction tools used for the analysis of the complete proteome. Signal peptide analysis by SignalP, TatP, TATFIND, FlaFind, and Duf361-Like programs revealed 35 proteins with SP1, five proteins with Tat signal, and two proteins with SP3 (Fig. 2 and supplemental Table 4A). The majority of proteins with SP1 are components of the ABC and TRAP transporter families. Five proteins identified with Tat motifs are the nitrate reductase α subunit; the Rieske iron-sulfur protein; the molybdopterin binding subunit of molybdopterin oxidoreductase; the hypothetical protein APE_0061.1, which is a cell surface-localized putative ABC

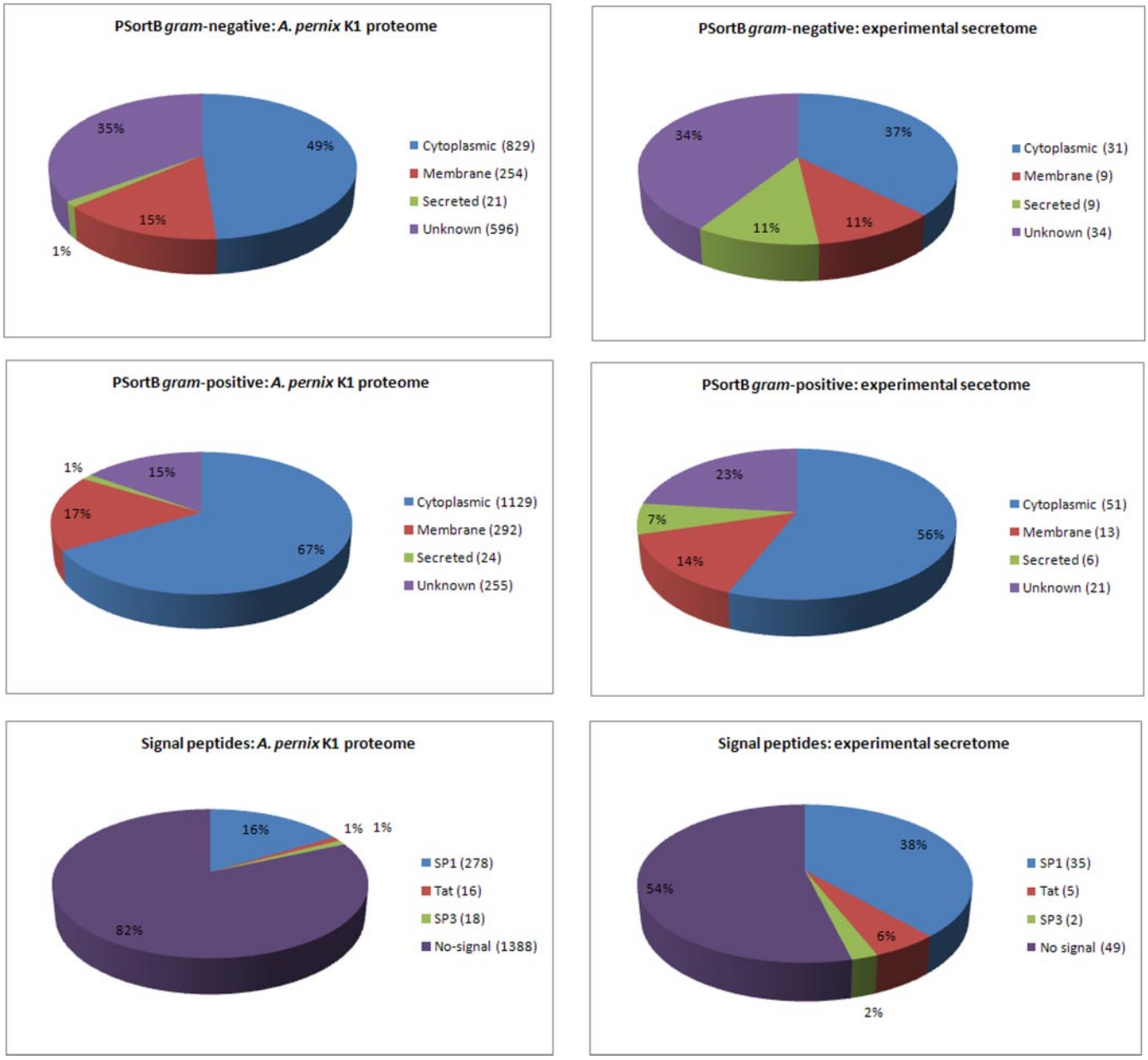

FIG. 2. **Graphical representation of protein localization sites as predicted by PSortB Gram-negative and Gram-positive programs and prediction of the possession of various signal peptides in the genome-translated *in silico* proteome of the *A. pernix* K1 containing 1700 proteins (*left side*; supplemental Table 3) and in the experimentally determined secretome of *A. pernix* consisting of 91 proteins (*right side*; supplemental Table 4).** *Numbers* in *parentheses* show the total number of proteins demonstrated to be positive for the given prediction.

sugar transporter subunit; and the MRP/NBP35 family protein (ABC transporter nucleotide-binding protein, surface fraction). The two SP3-bearing proteins (identified also as SP1), *i.e.* the spermidine/putrescine-binding protein and an "unknown" substrate-binding protein, are also components of ABC transporters. It should be noted that 50 proteins of the experimental secretome do not bear signal peptides recognized by these programs. These in part could be highly abundant cytoplasmic proteins contaminating the sample and in part proteins exported without a signal peptide and/or currently unknown mechanisms or both. By comparing the *A. pernix* K1 experimental secretome with that predicted *in silico* by PSortB (Fig. 2) 11 and 6 proteins of 21 and 24 predicted by the Gram-negative and -positive algorithms, respectively, were identified. This indicates that the PSortB gram-negative program could be more appropriate for archaeal secretome prediction. Twelve experimentally identified proteins were found to be secreted for at least one of the two PSortB analyses, and 13 were found to be secreted by non-classical mechanisms (SecP prediction; supplemental Table 4). Altogether, there are 18 proteins in the experimental data set predicted to be secreted using classical or non-classical mechanisms. By

TABLE III

Cell surface-exposed subunits of membrane transporters in the proteome of A. pernix K1

Protein name	Accession number	ORF	Family ID[a]	Transporter type[a]	TMS[b]	SP[c]	Sample[d]	Substrate
FeS assembly protein SufB	gi|14601570	APE_1703	ABC	ATP-dependent	0		ND	
ABC transporter, SBP	gi|118430849	APE_0035.1	ABC	ATP-dependent	0	SP1	S, E	Sugar
Hypothetical protein APE_0558.1	gi|118431107	APE_0558.1	ABC	ATP-dependent	0	SP1	S, E	Branched chain amino acid
ABC transporter, SBP	gi|118431555	APE_1688.1	ABC	ATP-dependent	0		S	Fe(III)
Phosphate ABC transporter, phosphate-binding protein	gi|14600404	APE_0045	ABC	ATP-dependent	1	SP1	S, E	Phosphate
Hypothetical protein APE_0061.1	gi|118430860	APE_0061.1	ABC	ATP-dependent	1	SP1, TatP	S, E	Sugar
Molybdate ABC transporter, molybdate-binding protein	gi|118430965	APE_0272.1	ABC	ATP-dependent	1	SP1	ND	Molybdenum
ABC transporter, SBP	gi|118430987	APE_0304.1	ABC	ATP-dependent	1	TatP	S, E	Oligopeptide
ABC transporter, SBP	gi|118431093	APE_0531.1	ABC	ATP-dependent	1	SP1	ND	Zinc/manganese ion
Putative ABC transporter, SBP	gi|118431313	APE_1049.1	ABC	ATP-dependent	1	SP1	S	Fe(III) dicitrate
ABC transporter, SBP	gi|118431402	APE_1303.1	ABC	ATP-dependent	1	SP1	S, E	Branched chain amino acid
ABC transporter, SBP	gi|118431437	APE_1390.1	ABC	ATP-dependent	1	SP1	E, S	Dipeptide
ABC transporter, SBP	gi|118431538	APE_1630.1	ABC	ATP-dependent	1	SP1, FlaFind	S	Sugar
ABC transporter, SBP	gi|14601589	APE_1728	ABC	ATP-dependent	1	SP1	E	Fe(III)/spermidine/putrescine
ABC transporter, SBP	gi|118431638	APE_1893.1	ABC	ATP-dependent	1	SP1	S	Glutamine
ABC transporter SBP	gi|118431798	APE_2254.1	ABC	ATP-dependent	1	SP1	E, S	Sugar
Dipeptide ABC transporter, dipeptide-binding protein	gi|14601949	APE_2257	ABC	ATP-dependent	1	SP1	E, S	Dipeptide/oligopeptide
ABC transporter, branched chain amino acid-binding protein	gi|118431910	APE_2521.1	ABC	ATP-dependent	1	SP1	S, E	Branched chain amino acid
Membrane lipoprotein family protein	gi|118431933	APE_2592.1	ABC	ATP-dependent	1	SP1	E, S	Ribose
ABC transporter, branched chain amino acid-binding protein	gi|14601070	APE_0917	ABC	ATP-dependent	2	SP1	E, S	Branched chain amino acid
Transporter, spermidine/putrescine-binding protein	gi|118431267	APE_0945.1	ABC	ATP-dependent	2	SP1, FlaFind	S	Spermidine/putrescine
ABC transporter, permease protein	gi|14601702	APE_1892	ABC	ATP-dependent	3		ND	Glutamine
MRP/NBP35 family protein nucleotide-binding domain[e]	gi|118430945	APE_0230.1	ABC	ATP-dependent	0	TatP	S	Nucleotide
ABC transporter, oligopeptide-binding protein[e]	gi|118431519	APE_1583.1	ABC	ATP-dependent	2	SP1	E, S	Oligopeptide
Arsenical pump-driving ATPase	gi|14601886	APE_2165	ArsAB	ATP-dependent	0		ND	Arsenite (ArsA homolog)
Arsenical pump-driving ATPase	gi|118431763	APE_2164.1	ArsAB	ATP-dependent	0		ND	Arsenite (ArsA homolog)
V-type ATP synthase subunit D	gi|118431024	APE_0402.1	F ATPase	ATP-dependent	0		S	Protons
V-type ATP synthase subunit A	gi|118431026	APE_0405.1	F ATPase	ATP-dependent	0		S	Protons
V-type ATP synthase subunit B	gi|118431025	APE_0404.1	F ATPase	ATP-dependent	0		S	Protons
V-type ATP synthase subunit K	gi|118431830	APE_2326.1	F ATPase	ATP-dependent	3	SP1	ND	Protons
Hypothetical protein APE_1552	gi|14601479	APE_1552	ClC	Secondary transporter	3	SP1	ND	Chloride ion
Twin arginine-targeting protein translocase	gi|118431755	APE_2154a	Tat	Secondary transporter	1	SP1	ND	Protein export
Twin arginine-targeting protein translocase	gi|118431746	APE_2139a	Tat	Secondary transporter	1	SP1	ND	Protein export
TRAP transporter, solute-binding component	gi|118431921	APE_2545.1	TRAP T	Secondary transporter	0	SP1	S	C_4-Dicarboxylate
TRAP transporter, solute-binding component	gi|118431744	APE_2136.1	TRAP T	Secondary transporter	1	SP1	E, S	C_4-Dicarboxylate
Putative mercury ion-binding protein	gi|118430838	APE_0009.1	MerTP	Unclassified	0		ND	Mercury
Small conductance mechanosensitive channel MscS	gi|118431624	APE_1867.1	MscS	Ion channels	3		S	Ion channel

[a] Family ID and transporter type according to the transporter classification system.

[b] Transmembrane segment calculated using TMHMM Server v.2.0.

[c] Signal peptide determined using SignalP, TatP, TATFIND, FlaFind, and Duf361-Like programs.

[d] S and E indicate the outer surface and exoprotein fractions, respectively, where the protein was identified. ND, not detected.

[e] These proteins are not present in TransportDB database.

reanalyzing all the identified proteins including the transmembrane and inner membrane-associated proteins (supplemental Table 4, A and B), 48 proteins (corresponding to 53% of the proteins identified in this work), however, had an unknown localization site for at least one of the two PSortB predictions, suggesting that unknown mechanisms are likely involved in archaeal protein secretion.

Cell Surface-exposed Subunits of Membrane Transporters in the Proteome of A. pernix K1—Membrane transport and outer membrane channel proteins carry ions and uncharged molecules of different chemical natures and of various sizes across the cell membrane. Carrier proteins and protein complexes identified in various organisms to date differ in membrane topology, energy coupling mechanism, and substrate specificity. In this work we analyzed the genome predicted membrane transporters of *A. pernix* K1 with particular attention to their solute-binding protein (SBP) components reported in the on-line accessible Transport DB database (42). By analyzing all the protein components of putative transporters (155 proteins), 37 membrane surface-exposed proteins possessing fewer than four transmembrane domains could be identified, and these are listed in Table III.

As the present study addressed the exoprotein and cell surface fractions, mainly the detection of the extracytoplasmic, cell surface-associated solute-binding receptors of transporters was expected. By analysis of the experimentally obtained secretome (91 proteins), we identified 26 transporter proteins (Table III). These belong to four transporter families: TRAP-T (two proteins), F-ATPase (two proteins), small conductance mechanosensitive ion channel (MscS) (one protein), and ABC (21 proteins). Proteins comprising the major part of these (21 of 24 predicted) are SBPs of the ABC superfamily, confirming that ABC-mediated transport represents the most frequent strategy adopted by *A. pernix* for solute translocation across the cell membrane. The high number of ABC SBPs in these samples also implies that the vast majority of the putative SBPs of ABC transporter systems were expressed under the culture conditions applied in this work. The majority of identified transporters possess signal peptides recognized by at least one of the signal peptide recognition programs used (supplemental Table 4). The most frequently occurring signal peptide is SP1, which suggests that Sec is the most extensively used secretion mechanism for SBPs of *A. pernix* K1. Two proteins with Tat motifs are hypothetical protein APE_0061.1 and the MRP/NBP35 family protein nucleotide-binding domain. SBP components of two ABC transporters with SP3, according to FlaFind prediction, could also be identified: spermidine/putrescine-binding protein precursor and ABC transporter substrate-binding protein. These proteins are secreted by the use of the type IV prepilin-like pathway. More interestingly, one ABC transporter solute-binding protein (APE_1688.1) and two members of the H^+- or Na^+-translocating V-type ATPase (APE_0404.1 and APE_0405.1) identified in the surface fraction did not possess signal peptides that could be identified by the prediction programs used.

In summary, by using an optimized membrane surface/extracellular protein purification procedure, SDS-PAGE separation, and nano-HPLC-ESI-MS/MS analysis, we identified 40 and 89 proteins in the exoprotein and surface fractions, respectively, of *A. pernix* K1. The membrane and inner membrane surface-associated proteins were subtracted from this set leading to formation of the experimental secretome containing 91 unique proteins that were then compared with the *in silico* predicted secretome. The analysis points out that secretion mechanisms in archaea can be only partially described by currently known mechanisms. Therefore, the experimentally determined protein data set may constitute a step forward for the setup of new archaea-specific prediction tools. In addition, in the exoprotein fraction a diverse arsenal of enzymes was expressed. Purification and enzymatic characterization of some of these are potentially interesting because of the hyperthermophilic nature of *A. pernix*.

[S] The on-line version of this article (available at http://www.mcponline.org) contains supplemental Tables 1–4.

‡ Both authors contributed equally to this work.

¶ To whom correspondence should be addressed: Inst. di Biochimica delle Proteine-Consiglio Nazionale delle Ricerche, via P. Castellino 111, 80131 Napoli, Italy. Tel.: 39-0816132570; Fax: 39-0816132277; E-mail: g.pocsfalvi@ibp.cnr.it.

REFERENCES

1. Woese, C. R., Kandler, O., and Wheelis, M. L. (1990) Towards a natural system of organisms: proposal for the domains archaea, bacteria, and eucarya. *Proc. Natl. Acad. Sci. U.S.A.* **87,** 4576–4579
2. Brochier-Armanet, C., Boussau, B., Gribaldo, S., and Forterre, P. (2008) Mesophilic crenarchaeota: proposal for a third archaeal phylum, the thaumarchaeota. *Nat. Rev. Microbiol.* **6,** 245–252
3. Koga, Y., and Morii, H. (2007) Biosynthesis of ether-type polar lipids in archaea and evolutionary considerations. *Microbiol. Mol. Biol. Rev.* **71,** 97–120
4. Sára, M., and Sleytr, U. B. (2000) S-layer proteins. *J. Bacteriol.* **182,** 859–868
5. Engelhardt, H. (2007) Are S-layers exoskeletons? The basic function of protein surface layers revisited. *J. Struct. Biol.* **160,** 115–124
6. Eichler, J. (2003) Facing extremes: archaeal surface-layer (glyco)proteins. *Microbiology* **149,** 3347–3351
7. Schäffer, C., and Messner, P. (2004) Surface-layer glycoproteins: an example for the diversity of bacterial glycosylation with promising impacts on nanobiotechnology. *Glycobiology* **14,** 31R–42R
8. Näther, D. J., Rachel, R., Wanner, G., and Wirth, R. (2006) Flagella of *Pyrococcus furiosus*: multifunctional organelles, made for swimming, adhesion to various surfaces, and cell-cell contacts. *J. Bacteriol.* **188,** 6915–6923
9. Moissl, C., Rachel, R., Briegel, A., Engelhardt, H., and Huber, R. (2005) The unique structure of archaeal hami, highly complex cell appendages with nano-grappling hooks. *Mol. Microbiol.* **56,** 361–370
10. Albers, S. V., Szabó, Z., and Driessen, A. J. (2006) Protein secretion in the archaea: multiple paths towards a unique cell surface. *Nat. Rev. Microbiol.* **4,** 537–547
11. Szabó, Z., Stahl, A. O., Albers, S. V., Kissinger, J. C., Driessen, A. J., and Pohlschröder, M. (2007) Identification of diverse archaeal proteins with class III signal peptides cleaved by distinct archaeal prepilin peptidases. *J. Bacteriol.* **189,** 772–778
12. Pohlschröder, M., Giménez, M. I., and Jarrell, K. F. (2005) Protein transport in archaea: Sec and twin arginine translocation pathways. *Curr. Opin. Microbiol.* **8,** 713–719

13. Ng, S. Y., Chaban, B., VanDyke, D. J., and Jarrell, K. F. (2007) Archaeal signal peptidases. *Microbiology* **153,** 305–314
14. Bardy, S. L., Eichler, J., and Jarrell, K. F. (2003) Archaeal signal peptides—a comparative survey at the genome level. *Protein Sci.* **12,** 1833–1843
15. Saleh, M., Song, C., Nasserulla, S., and Leduc, L. G. (2009) Indicators from archaeal secretomes. *Microbiol. Res.*, Epub ahead of print, PubMed PMID: 18407482
16. Albers, S. V., Koning, S. M., Konings, W. N., and Driessen, A. J. (2004) Insights into ABC transport in archaea. *J. Bioenerg. Biomembr.* **36,** 5–15
17. Sako, Y., Nomura, N., Uchida, A., Ishida, Y., Morii, H., Koga, Y., Hoaki, T., and Maruyama, T. (1996) Aeropyrum pernix gen. nov., sp. nov., a novel aerobic hyperthermophilic archaeon growing at temperatures up to 100 degrees C. *Int. J. Syst. Bacteriol.* **46,** 1070–1077
18. Morii, H., Yagi, H., Akutsu, H., Nomura, N., Sako, Y., and Koga, Y. (1999) A novel phosphoglycolipid archaetidyl(glucosyl)inositol with two sesterterpanyl chains from the aerobic hyperthermophilic archaeon *Aeropyrum pernix* K1. *Biochim. Biophys. Acta* **1436,** 426–436
19. Yamazaki, S., Yamazaki, J., Nishijima, K., Otsuka, R., Mise, M., Ishikawa, H., Sasaki, K., Tago, S., and Isono, K. (2006) Proteome analysis of an aerobic hyperthermophilic crenarchaeon, *Aeropyrum pernix* K1. *Mol. Cell. Proteomics* **5,** 811–823
20. Laemmli, U. K. (1970) Cleavage of structural proteins during the assembly of the head of bacteriophage T4. *Nature* **227,** 680–685
21. Shevchenko, A., Wilm, M., Vorm, O., and Mann, M. (1996) Mass spectrometric sequencing of proteins silver-stained polyacrylamide gels. *Anal. Chem.* **68,** 850–858
22. Keller, A., Nesvizhskii, A. I., Kolker, E., and Aebersold, R. (2002) Empirical statistical model to estimate the accuracy of peptide identifications made by MS/MS and database search. *Anal. Chem.* **74,** 5383–5392
23. Bendtsen, J. D., Nielsen, H., von Heijne, G., and Brunak, S. (2004) Improved prediction of signal peptides: SignalP 3.0. *J. Mol. Biol.* **340,** 783–795
24. Bendtsen, J. D., Kiemer, L., Fausbøll, A., and Brunak, S. (2005) Non-classical protein secretion in bacteria. *BMC Microbiol.* **5,** 58
25. Bendtsen, J. D., Nielsen, H., Widdick, D., Palmer, T., and Brunak, S. (2005) Prediction of twin-arginine signal peptides. *BMC Bioinformatics* **6,** 167
26. Juncker, A. S., Willenbrock, H., Von Heijne, G., Brunak, S., Nielsen, H., and Krogh, A. (2003) Prediction of lipoprotein signal peptides in Gram-negative bacteria. *Protein Sci.* **12,** 1652–1662
27. Krogh, A., Larsson, B., von Heijne, G., and Sonnhammer, E. L. (2001) Predicting transmembrane protein topology with a hidden Markov model: application to complete genomes. *J. Mol. Biol.* **305,** 567–580
28. Gardy, J. L., Laird, M. R., Chen, F., Rey, S., Walsh, C. J., Ester, M., and Brinkman, F. S. L. (2005) PSORTb v. 2.0: Expanded prediction of bacterial protein subcellular localization and insights gained from comparative proteome analysis. *Bioinformatics* **21,** 617–623
29. Rose, R. W., Brüser, T., Kissinger, J. C., and Pohlschröder, M. (2002) Adaptation of protein secretion to extremely high-salt conditions by extensive use of the twin-arginine translocation pathway. *Mol. Microbiol.* **45,** 943–950
30. Mulkidjanian, A. Y., Makarova, K. S., Galperin, M. Y., and Koonin, E. V. (2007) Inventing the dynamo machine: the evolution of the F-type and V-type ATPases. *Nat. Rev. Microbiol.* **5,** 892–899
31. vanden Hoven, R. N., and Santini, J. M. (2004) Arsenite oxidation by the heterotrophy hydrogenophaga sp. str. NT-14: the arsenite oxidase and its physiological electron acceptor. *Biochim. Biophys. Acta* **1656,** 148–155
32. Cabello, P., Roldán, M. D., and Moreno-Vivián, C. (2004) Nitrate reduction and the nitrogen cycle in archaea. *Microbiology* **150,** 3527–3546
33. Ring, G., and Eichler, J. (2004) In the archaea *Haloferax volcanii*, membrane protein biogenesis and protein synthesis rates are affected by decreased ribosomal binding to the translocon. *J. Biol. Chem.* **279,** 53160–53166
34. Bisle, B., Schmidt, A., Scheibe, B., Klein, C., Tebbe, A., Kellermann, J., Siedler, F., Pfeiffer, F., Lottspeich, F., and Oesterhelt, D. (2006) Quantitative profiling of the membrane proteome in a halophilic archaeon. *Mol. Cell. Proteomics* **5,** 1543–1558
35. Son, H. J., Shin, E. J., Nam, S. W., Kim, D. E., and Jeon, S. J. (2007) Properties of the α subunit of a chaperonin from the hyperthermophilic crenarchaeon *Aeropyrum pernix* K1. *FEMS Microbiol. Lett.* **266,** 103–109
36. Trent, J. D., Kagawa, H. K., Paavola, C. D., McMillan, R. A., Howard, J., Jahnke, L., Lavin, C., Embaye, T., and Henze, C. E. (2003) Intracellular localization of a group II chaperonin indicates a membrane-related function. *Proc. Natl. Acad. Sci. U.S.A.* **100,** 15589–15594
37. Pocsfalvi, G., Cacace, G., Cuccurullo, M., Serluca, G., Sorrentino, A., Schlosser, G., Blaiotta, G., and Malorni, A. (2008) Proteomic analysis of exoproteins expressed by enterotoxigenic *Staphylococcus aureus* strains. *Proteomics* **8,** 2462–2476
38. Halio, S. B., Blumentals, I. I., Short, S. A., Merrill, B. M., and Kelly, R. M. (1996) Sequence, expression in *Escherichia coli*, and analysis of the gene encoding a novel intracellular protease (Pfpl) from the hyperthermophilic archaeon *Pyrococcus furiosus*. *J. Bacteriol.* **178,** 2605–2612
39. Catara, G., Ruggiero, G., La Cara, F., Digilio, F. A., Capasso, A., and Rossi, M. (2003) A novel extracellular subtilisin-like protease from the hyperthermophile *Aeropyrum pernix* K1: biochemical properties, cloning, and expression. *Extremophiles* **7,** 391–399
40. Ishikawa, K., Ishida, H., Koyama, Y., Kawarabayasi, Y., Kawahara, J., Matsui, E., and Matsui, I. (1998) Acylamino acid-releasing enzyme from the thermophilic archaeon *Pyrococcus horikoshii*. *J. Biol. Chem.* **273,** 17726–17731
41. Kawarabayasi, Y., Hino, Y., Horikawa, H., Yamazaki, S., Haikawa, Y., Jin-no, K., Takahashi, M., Sekine, M., Baba, S., Ankai, A., Kosugi, H., Hosoyama, A., Fukui, S., Nagai, Y., Nishijima, K., Nakazawa, H., Takamiya, M., Masuda, S., Funahashi, T., Tanaka, T., Kudoh, Y., Yamazaki, J., Kushida, N., Oguchi, A., Aoki, K., Kubota, K., Nakamura, Y., Nomura, N., Sako, Y., and Kikuchi, H. (1999) Complete genome sequence of an aerobic hyperthermophilic crenarchaeon, *Aeropyrum pernix* K1. *DNA Res.* **6,** 83–101, 145–152
42. Ren, Q., Chen, K., and Paulsen, I. T. (2007) TransportDB: a comprehensive database resource for cytoplasmic membrane transport systems and outer membrane channels. *Nucleic Acids Res.* **35,** D274–D279